Isı Bilimi ve Tekniği Dergisi, 44, 1, 17-31, 2024
J. of Thermal Science and Technology
©2024 TIBTD Printed in Turkey
ISSN 1300-3615
e-ISSN 2667-7725
https://doi.org/10.47480/isibted.1493766

ENERGY AND ENVIRONMENTAL ASSESSMENT OF CO_2 BOOSTER REFRIGERATION CYCLES WITH FLOODED EVAPORATORS AND PARALLEL COMPRESSOR FOR SUPERMARKETS IN TÜRKİYE

Nagihan BİLİR SAĞ*, Metehan IŞIK**
*Konya Teknik Üniversitesi Mühendislik ve Doğa Bilimleri Fakültesi Makina Mühendisliği Bölümü
42250 Selçuklu, Konya, nbilir@ktun.edu.tr ORCID: 0000-0001-8410-0268
** Konya Teknik Üniversitesi Mühendislik ve Doğa Bilimleri Fakültesi Makina Mühendisliği Bölümü
42250 Selçuklu, Konya, misik@ktun.edu.tr ORCID: 0000-0002-0044-2701

(Geliş Tarihi: 28.02.2023, Kabul Tarihi: 11.03.2024)

Abstract: CO_2 booster refrigeration systems have higher energy efficiency and are more environmentally friendly. Therefore, the CO_2 booster refrigeration cycle with flooded evaporators and parallel compressors (BFP), BFP with mechanical subcooling (BFP-MSC), and BFP with evaporative cooling (BFP-EVC) are investigated for supermarkets in this study. For the first time in the literature, these systems are analyzed to present which system performs better in terms of energy and environmental performance for Türkiye. According to the results of the investigation, BFP-MSC has a better coefficient of performance (COP) values than BFP, with up to a 16.67% increase at equivalent dry bulb temperatures. Meanwhile, BFP-EVC has the lowest annual energy consumption (AEC) in each city, followed by BFP-MSC and then BFP. Annual savings obtained by BFP-EVC over BFP vary between 10.81% to 25.47%. Additionally, BFP-EVC offers more substantial savings in cities with lower humidity levels, as it was analyzed with respect to wet bulb temperatures.
Keywords: Booster systems, CO_2, Energetic analysis, Environmental analysis, Supermarket refrigeration.

TÜRKİYE'DEKİ SÜPERMARKETLER İÇİN YAŞ EVAPORATÖRLÜ VE PARALEL KOMPRESÖRLÜ CO_2 BOOSTER SOĞUTMA ÇEVRİMLERİNİN ENERJİ VE ÇEVRE ANALİZİ

Özet: CO_2 booster soğutma sistemleri yüksek enerji verimliliğine sahip olup çevre dostudur. Bu nedenle, bu çalışmada süpermarketler için CO_2 akışkanlı yaş evaporatörlü ve paralel kompresörlü soğutma çevrimi (BFP), BFP'ye mekanik aşırı soğutma eklenen soğutma çevrimi (BFP-MSC) ve BFP'de buharlaşmalı soğutma kullanılan soğutma çevrimi (BFP-EVC) incelenmiştir. Bu sistemler analiz edilerek enerji ve çevre performansı açısından hangi sistemin daha iyi performans gösterdiği literatürde ilk kez Türkiye'deki süpermarketler için ortaya konulmuştur. Araştırma sonuçlara göre, BFP-MSC'nin aynı kuru termometre sıcaklıklarında BFP'ye göre %16.67'ye kadar daha yüksek soğutma performans katsayısına (COP) sahip olduğu belirlenmiştir. Bunun yanı sıra, her şehirde BFP-EVC, en düşük yıllık enerji tüketimine (AEC) sahiptir, onu BFP-MSC ve ardından BFP takip etmektedir. BFP-EVC'nin BFP'ye göre sağladığı yıllık tasarruf %10.81 ile %25.47 arasında değişmektedir. Ek olarak, BFP-EVC, yaş termometre sıcaklıklarına bağlı olarak analiz edildiği için, nem oranının düşük olduğu şehirlerde daha yüksek tasarruflar sağlamaktadır.
Anahtar Kelimler: Booster sistemleri, CO_2, Enerji analizi, Çevre analizi, Süpermarket soğutma.

NOMENCLATURE

1, 2…	refrigerant state points
α	recycling factor
add	additional
AEC	annual energy consumption
amb	ambient
BFP	booster refrigeration cycle with flooded evaporators and parallel compressor
Comp	compressor
cond	condenser
COP	coefficient of performance
DBT	dry bulb temperature
EES	engineering equation solver
η	overall compressor efficiency
EVC	evaporative cooling
FGBV	flash gas bypass valve
gc	gas cooler
GWP	global warming potential
h	specific enthalpy (kJ/kg)
HS	high stage
IHX	internal heat exchanger
LS	low stage
LT	low temperature
LVS	liquid/vapor separator
ṁ	mass flow rate (kg/s)
MSC	mechanical subcooling

MT	medium temperature
n	total operation time (years)
P	pressure (kPa)
PAR	parallel compressor
$\dot{Q}$	cooling capacity, heat rejection (kW)
R	ratio
RC	regional electricity conversion factor
SC	sub cooler
T	temperature (°C)
$\dot{W}$	energy consumption (kW)
WBT	wet bulb temperature
x	quality

INTRODUCTION

The use of CO_2 as a refrigerant in supermarket refrigeration systems attracts attention with its thermophysical properties and nature-friendly behavior (Gullo et al., 2018). However, CO_2 refrigeration systems have some difficulties such as higher equipment costs because of CO_2's high working pressures (Goetzler et al., 2014) and critical temperature of CO_2 which is 30.98 °C causing CO_2 systems to operate transcritical (heat rejection at supercritical zone). In the literature review, there are studies dealing with the use and improvement of CO_2 refrigeration systems both theoretically (Ersoy and Bilir, 2012; Ge et al., 2015; Gullo and Hafner, 2017; Mylona et al., 2017; Sarkar and Agrawal, 2010; Sawalha, 2008a, 2008b) and experimentally (Chesi et al., 2014; Fricke et al., 2016; Fritschi et al., 2017; Llopis, Sanz-Kock, et al., 2015; Nebot-Andrés et al., 2021). Alongside these studies focusing on the improvement of the systems, there are also city-based studies (Cui et al., 2020; Gullo et al., 2016; Işık, 2022; Karampour and Sawalha, 2018; Lata et al., 2021; Mitsopoulos et al., 2019; Sooben et al., 2019; Tsamos et al., 2017) to show the outcomes when they are used in supermarkets in daily operations.

The literature on CO_2 transcritical refrigeration systems encompasses a wide range of studies aimed at both understanding the key parameters influencing their performance and enhancing their overall efficiency. While some researchers have delved into understanding the aspects of these systems, others have focused on innovations to improve their functionality. Notably, modifications to the classical one-evaporator cycle have been explored, including the incorporation of auxiliary compressors, two-stage compressors, and internal heat exchangers. Additionally, researchers have examined the expansion process, exploring alternatives such as ejectors (Atmaca et al., 2018) or turbines (Bayrakçı et al., 2014). For instance, Bayrakçı et al. (2014) demonstrated that the utilization of a turbine can lead to a remarkable 10% increase in performance. However, a unique challenge arises in the context of supermarket refrigeration systems, where the need for two evaporator stages, catering to both fresh and frozen food sections, necessitates innovative solutions to adapt CO_2 refrigeration systems for optimal use in this specific application. This ongoing research strives to address the complex demands of supermarket refrigeration while maximizing the benefits of CO_2 transcritical technology. According to studies in the literature, booster refrigeration systems come to the fore as they can meet the two temperature levels (low temperature and medium temperature) refrigeration needs of supermarkets in one single cycle with higher efficiency than traditional systems (European Commission, 2008; Mylona et al., 2017). Moreover, booster systems have lower annual energy consumption (AEC) when compared to R404A systems (Cui et al., 2020), which are frequently used in supermarket refrigeration (ICF Incorporated, 2020). This outcome has been presented in the literature by city-based studies by annual performance metrics for various climatic conditions. Several studies have highlighted the advantages of booster refrigeration systems over traditional R404A systems in terms of energy consumption. Mitsopoulos et al. (2019) have conducted research in Athens and found that some types of booster systems consumed less energy annually. Similarly, Gullo et al.'s (2016) study in cities like Valencia and Seville has yielded similar results, further emphasizing the superiority of booster systems in reducing energy consumption. Cui et al.'s (2020) examination of these refrigeration systems in five Chinese cities has revealed that energy savings were primarily observed in the coldest city, suggesting that booster systems may require further enhancements to optimize performance in warmer climates. These findings underscore the need for continued research and development to adapt booster systems for a wider range of environmental conditions.

The use of flooded evaporators has been presented in the literature as a method that increases energy savings for warmer climates. In the study of Karampour and Sawalha (2018), approximately 12% annual energy savings have been shown when both cooling level evaporators are flooded for Barcelona and Stockholm. Up to 155.1 MWh energy savings have been demonstrated for Indian context (Lata et al., 2021) and more than 10% annual energy efficiency ratio improvement over standard CO_2 booster refrigeration system have been shown for China by using flooded evaporators (Cui et al., 2020).

There are also studies considering the use of parallel compressors (Amaris et al., 2019; Caliskan and Ersoy, 2022; Dai et al., 2022), which is a step towards reducing the power consumed by the high-pressure compressor in booster refrigeration cycles. Besides Sacasas et al.'s (2022) study for Chile has shown that CO_2 booster systems with parallel compressors consume less energy than standard booster systems, similar results have been revealed for New Delhi, Seville, Phoenix, and Teheran (Purohit et al., 2017). Energy savings have also been obtained in Athens, London (Tsamos et al., 2017) and Chinese cities (Sun et al., 2020) with CO_2 booster systems with parallel compressor. Furthermore, the best annual energy efficiency ratios have been obtained for the CO_2 booster refrigeration cycle with flooded evaporators and parallel compressor (BFP) for all 5 cities considered in the study of Cui et al. (2020). Accordingly, the most energy savings have been achieved with the

BFP in Stockholm and Barcelona (Karampour and Sawalha, 2018) and 12 cities of Türkiye (Işık, 2022; Işık and Bilir Sağ, 2023). Although only medium temperature evaporator is flooded, the BFP has presented the lowest AEC for Rome, Valencia, and Seville (Gullo et al., 2016).

The application of mechanical subcooling as a modification to the booster systems has also been exhibited as advantageous in the literature. While Cui et al. (2020) have presented mechanical subcooling increases annual energy efficiency ratios for Chinese example, annual energy savings of 3% for Stockholm and 7.5% for Barcelona have been provided by mechanical subcooling in the standard CO_2 booster cycle (Karampour and Sawalha, 2018). In these two studies, the mechanical subcooling cycle used R290 as a refrigerant. In the study of Llopis et al. (2015) for one stage CO_2 refrigeration cycles, COP improvement percentages have shown almost the same according to different subcooling cycle refrigerants such as R290, R1270, R1234yf, R161, R512a, and R134a. To get rid of the negative effects of high ambient temperatures, an advantage can be provided for refrigeration systems by evaporative cooling (Lata and Gupta, 2020; Sooben et al., 2019). These systems are based on the evaporation of water to reduce the temperature of air, where the gas cooler/condenser releases heat. In the study of Lata et al. (2021), it has been shown that annual energy savings are achieved in the range of 120.2 MWh - 238.6 MWh for the standard CO_2 booster cycle with evaporative cooling, and in the range of 103.2 MWh - 205.9 MWh when evaporative cooling has been performed in the CO_2 booster refrigeration cycle with flooded evaporators.

According to recent studies, CO_2 booster systems are an energy-efficient and eco-friendly beneficial option, particularly for usage in supermarket refrigeration. This is especially significant in countries with many supermarkets, such as Türkiye. Türkiye is also dedicated to reducing CO_2 emissions in the future, emphasizing the importance of CO_2 booster systems. Additionally, due to the diverse climates of Türkiye's cities, it is essential to investigate CO_2 booster systems and their environmental effects in a variety of outdoor conditions. Therefore, three systems have been investigated in this study for the first time in the open literature, to the best of the authors' knowledge: the CO_2 booster refrigeration cycle with flooded evaporators and parallel compressors (BFP), the BFP with mechanical subcooling (BFP-MSC), and the BFP with evaporative cooling (BFP-EVC). The aim is to determine which of these systems performs better in terms of both energy efficiency and environmental effect across nine Türkiye cities.

CO_2 BOOSTER REFRIGERATION CYCLE WITH FLOODED EVAPORATORS AND PARALLEL COMPRESSOR

The schematic diagrams of systems examined in this study are given in this section with their P-h diagrams. The basis system in this study is the CO_2 booster refrigeration cycle with flooded evaporators and parallel compressor (BFP) shown in Fig. 1. BFP was chosen as the main system as it has previously been shown the most energy saving system for supermarkets of Türkiye when compared to booster systems without flooded evaporators or parallel compressor (Işık and Bilir Sağ, 2023). The other two systems have modifications on that BFP basis.

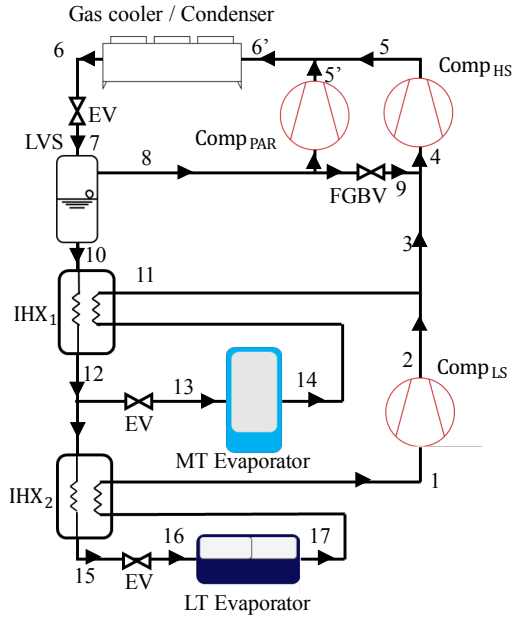

(a)

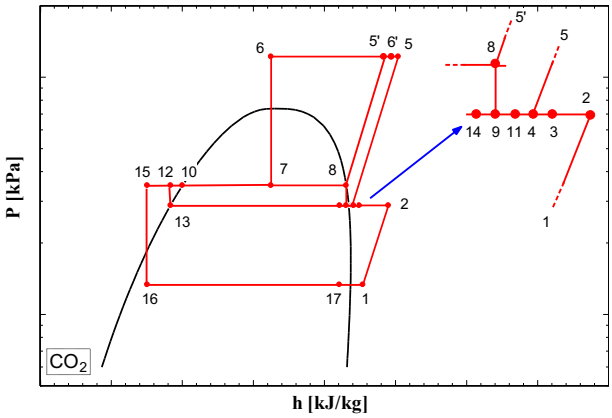

(b)

Fig. 1. The schematic (a) and P-h diagram (b) of the BFP.

In the BFP, CO_2 entering the gas cooler (condenser when it is a subcritical operation) rejects heat to the environment between points 5 and 6. The refrigerant is then throttled at the expansion valve (EV). The refrigerant, whose pressure and temperature are reduced, is divided as saturated liquid and saturated vapor at liquid-vapor separator (LVS). The saturated vapor of the separated refrigerant enters the flash gas bypass valve (FGBV) at point 8, while the saturated liquid proceeds to the internal heat exchangers (IHX) before the medium temperature (MT) and low temperature (LT) evaporators. In IHX 2, heat is transferred from saturated liquid CO_2 to saturated mixture CO_2 coming from MT evaporator. Similarly, in IHX 2, CO_2 coming from LT evaporator takes heat from compressed liquid CO_2 on the other side

of the heat exchanger. As a result, the quality of refrigerant entering the evaporators is decreased while the superheated vapor state of refrigerant is provided for compressors to operate appropriately.

The refrigerant taking heat from the frozen food cabinet between points 16 and 17 leaves the IHX 1 as superheated vapor at state 1 and is compressed in the low stage compressor ($Comp_{LS}$) to state 2. On the other hand, the fresh food cabinet is cooled by MT evaporator where refrigerant leaves the evaporator at state 14. It exits IHX 1 as state 11 and reaches state 3 by mixing with the refrigerant at state 2. The refrigerant at point 3 and the refrigerant exiting the FGBV at point 9 mix and enter the high stage compressor ($Comp_{HS}$) in the state point 4 to be compressed. Finally, the refrigerant enters the gas cooler, and the cycle continues.

When the parallel compressor is active, the refrigerant from the LVS does not enter the FGBV and is compressed in the parallel compressor ($Comp_{PAR}$). In this case, the CO_2 at state 3 enters $Comp_{HS}$ directly. The refrigerant comes out of the $Comp_{HS}$ and $Comp_{PAR}$ mix and enters the gas cooler to complete the cycle.

In this system, LVS and the use of FGBV equipment between points 8-9 are providing refrigerant to enter the evaporators with a high saturated liquid ratio and flooded evaporators provide lower quality and more wet surface for evaporators. Also, $Comp_{PAR}$ reduces the work done by $Comp_{HS}$.

Mechanical subcooling (MSC) and evaporative cooling (EVC) are the selected modifications to improve the BFP system. The schematic diagram and P-h diagram of BFP-MSC are demonstrated in Fig. 2 while Fig. 3 shows BFP-EVC's diagrams.

The integration of a mechanical subcooling cycle, positioned at the outlet of the gas cooler/condenser, plays a pivotal role in enhancing the performance of this refrigeration system. This innovative addition effectively reduces the quality of the refrigerant entering the liquid-vapor separator (LVS) by the transfer of heat from CO_2 to R290 in the subcooler (SC). Consequently, this reduction in refrigerant quality leads to decreased vapor mass flow rates at LVS and a subsequent reduction in the work done by the compressors. This improvement is crucial for achieving energy savings and enhancing the performance of the refrigeration system.

In the BFP-EVC system, a key strategy for reducing the temperature of the air involves employing evaporative cooling until it reaches the wet bulb temperature. This approach yields a significant advantage as the wet bulb temperature consistently registers lower values than the dry bulb temperature. Consequently, the BFP-EVC system exhibits lower power consumption compared to the BFP system operating at the same dry bulb temperature. Lower operating temperatures provide lower inlet quality for LVS, leading to a reduction in the mass flow rates within the system.

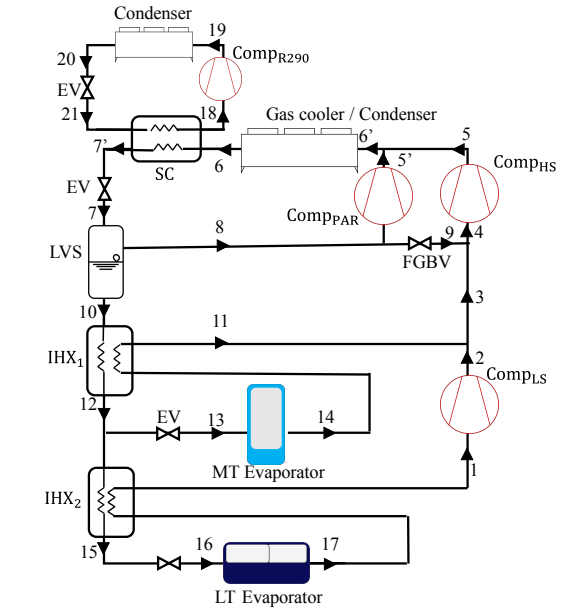

(a)

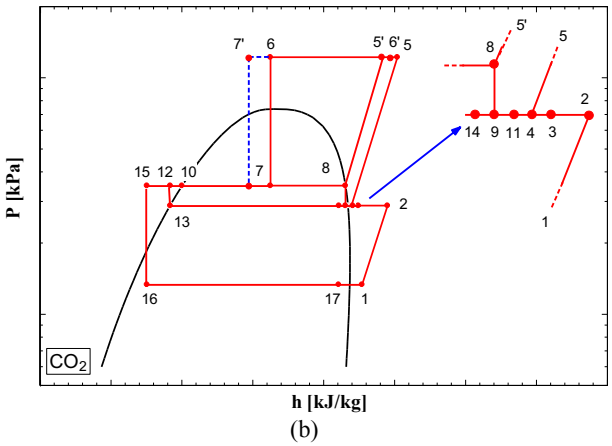

(b)

Fig. 2. a) Schematic diagram and b) P-h diagram of BFP-MSC.

MATHEMATICAL MODELING

Energy Analysis Model

For energy analysis, cities with different climates from different geographical regions of Türkiye are selected and the annual energy consumption (AEC) results of the systems in question are examined.
Ambient temperatures are divided as Subcritical 1, Subcritical 2, Transition, and Transcritical operating zones (Table 1) (Cui et al., 2020; Mitsopoulos et al., 2019). While subcritical operation occurs with saturation conditions, gas cooler pressure at transcritical operation zone has an optimum value (Kauf, 1999; Liao et al., 2000; Özgür et al., 2009) calculated by the Engineering Equation Solver (EES). Values for Transition zone are assumed to have a linear change between Subcritical 2 and Transcritical zones.

The cooling capacity of the low temperature (LT) evaporator for frozen foods is taken as 35 kW (Karampour and Sawalha, 2018) at -32 ℃ evaporator temperature, (Gullo et al., 2016) while the cooling capacity of the medium temperature (MT) evaporator to be used in the preservation of fresh foods is taken as 165 kW at -7 ℃ evaporator temperature (Cui et al., 2020) as this load is the average for Türkiye (Işık, 2022).

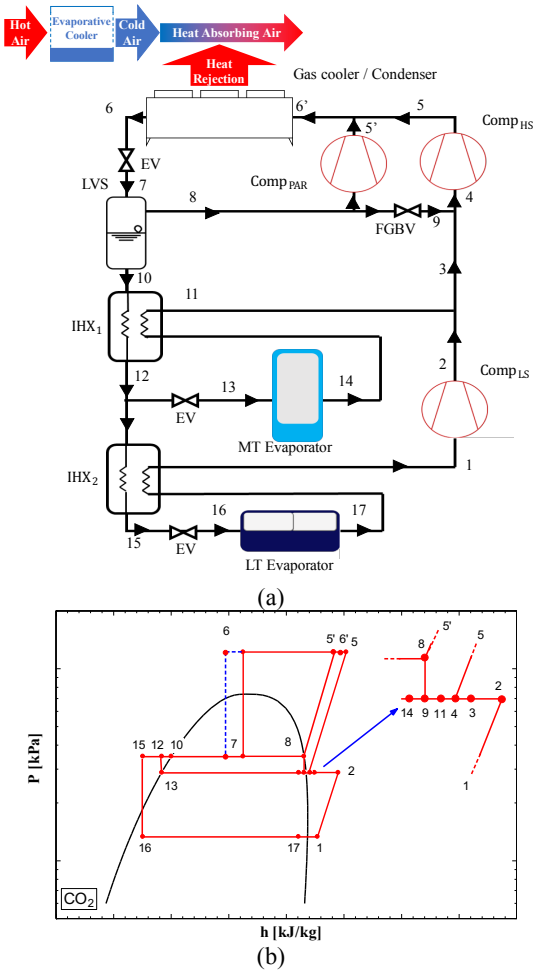

Fig. 3. a) Schematic diagram and b) P-h diagram of BFP-EV

In the CO_2 booster refrigeration cycle with flooded evaporators, parallel compressor and mechanical subcooling (BFP-MSC), the temperature of the CO_2 leaving the gas cooler is reduced by the mechanical subcooling cycle. In this way, CO_2 releases heat, and the quality of the refrigerant entering the liquid vapor separator (LVS) is reduced. The activation of the parallel compressor starts when the ambient temperature is 14°C due to getting enough vapor for the auxiliary compressor (Mitsopoulos et al., 2019). The mechanical subcooling starts at the ambient temperature of 19°C (Cui et al., 2020). As a result of the reduction in quality of the refrigerant entering the LVS with subcooling, the parallel compressor goes out of its proper operating range and shuts down. Then it is activated again at 29 ℃ ambient temperature and operates together with mechanical subcooling as given in Table 2.

The assumptions done for the mathematical model are as follows:

- Heat losses and pressure drops in the heat exchangers and pipes are neglected.
- It is assumed that all expansion valves perform isenthalpic processes.
- The CO_2 flooded evaporator outlet vapor quality is accepted as 0.95 (Cui et al., 2020).
- Intermediate pressure is assumed to be 3500 kPa (Cui et al., 2020; Gullo et al., 2016; Tsamos et al., 2017).
- IHX effectiveness is taken 0.65 (Cui et al., 2020).
- R290 evaporator temperature is 10 ℃ with 10 ℃ superheat (Cui et al., 2020).
- R290 condenser temperature is 10 ℃ higher than the ambient temperature (Cui et al., 2020).
- Evaporative cooling occurs until saturation (ambient temperatures assumed as wet bulb temperatures)(Lata and Gupta, 2020).
- Additional work ($\dot{W}_{add}$)(fans etc.) is assumed 3% of the heat rejected from gas cooler/condenser (Cui et al., 2020).

Table 1. Pressure and temperature values due to ambient temperature operating zones.

Operating Zones	Ambient Temperature Ranges (℃)	Gas cooler outlet/condenser temperature (℃)	Gas cooler /condenser pressure (kPa)
Subcritical 1(Cui et al., 2020)	$T_{amb} < 2$	10	P_{sat}@10 ℃
Subcritical 2(Cui et al., 2020)	$2 \leq T_{amb} < 14$	$T_{amb} + 8$	P_{sat}@T_{cond}
Transition	$14 \leq T_{amb} < 28$	$0.642\ T_{amb} + 13.007$	$98.283\ T_{amb} + 4627.03$
Transcritical	$28 \leq T_{amb}$	$T_{amb} + 3$	optimized

Table 2. Activation temperatures of parallel compressor and mechanical subcooling for systems.

Systems	Parallel Compressor	Mechanical Subcooling	Reference
BFP	$14 \leq T_{amb}$	-	(Mitsopoulos et al., 2019)
BFP-MSC	$14 \leq T_{amb} < 18$ $29 \leq T_{amb}$	$19 \leq T_{amb}$	(Cui et al., 2020)
BFP-EVC	$14 \leq T_{amb}$	-	(Mitsopoulos et al., 2019)

After determining all operating zones, operating conditions, and assumptions, COP and power consumption values are calculated as the following procedure explained below.

Conservation of mass and energy laws are applied at all calculations. Mass flow rates are determined as given below for LVS for all systems considered in this study:

$$\dot{m}_8 = \dot{m}_7 x_7 \quad (1)$$

$$\dot{m}_{10} = \dot{m}_7 (1 - x_7) \quad (2)$$

$$\dot{m}_7 = \dot{m}_8 + \dot{m}_{10} \quad (3)$$

Heat exchanger energy balances are calculated by Eqn. (4) and Eqn. (5).

$$\dot{m}_{10}(h_{10} - h_{12}) = \dot{m}_{13}(h_{11} - h_{14}) \quad (4)$$

$$h_{12} - h_{15} = h_1 - h_{17} \quad (5)$$

Energy balances at mixing points are presented as:

$$\dot{m}_3 h_3 = \dot{m}_2 h_2 + \dot{m}_{11} h_{11} \quad (6)$$

$$\dot{m}_4 h_4 = \dot{m}_3 h_3 + \dot{m}_9 h_9 \quad (7)$$

$$\dot{m}_{6'} h_{6'} = \dot{m}_5 h_5 + \dot{m}_{5'} h_{5'} \quad (8)$$

In MSC cycle, the heat rejected by CO_2 is absorbed by R290 refrigerant within the subcooler. Energy balance of this process is given by Eqn. (10). The CO_2 is subcooled 10 ℃ after the gas cooler/condenser before entering LVS (Cui et al., 2020).

$$\dot{m}_{18}(h_{18} - h_{21}) = \dot{m}_{6'}(h_6 - h_{7'}) \quad (10)$$

MT and LT evaporator loads are calculated by the following equations.

$$\dot{Q}_{LT} = \dot{m}_{16} * (h_{17} - h_{16}) \quad (11)$$

$$\dot{Q}_{MT} = \dot{m}_{13} * (h_{14} - h_{13}) \quad (12)$$

The heat rejected from CO_2 gas cooler/condenser is calculated with Eqn. (13).

$$\dot{Q}_{gc/cond} = \dot{m}_{6'} * (h_{6'} - h_6) \quad (13)$$

Power consumption value of low stage compressor is calculated as given in Eqn. (14) as its overall efficiency is calculated by Eqn. (15) related with compression ratio. All overall efficiency correlations are taken from the study of Cui et al.(2020).

$$\dot{W}_{Comp_{LS}} = \frac{\dot{m}_1 * (h_{2,s} - h_1)}{\eta_{Comp_{LS}}} \quad (14)$$

$$\eta_{Comp_{LS}} = -0.0111 R_{P,LS}^2 + 0.0793 R_{P,LS} + 0.8030 \quad (15)$$

Similar to low stage, high stage compressor and parallel compressor's power consumptions are obtained as follows:

$$\dot{W}_{Comp_{HS}} = \frac{\dot{m}_5 * (h_{5,s} - h_4)}{\eta_{Comp_{HS}}} \quad (16)$$

$$\eta_{Comp_{HS}} = -0.01 R_{P,HS}^2 + 0.0468 R_{P,HS} + 0.6134 \quad (17)$$

$$\dot{W}_{Comp_{PAR}} = \frac{\dot{m}_{5'} * (h_{5',s} - h_8)}{\eta_{Comp_{PAR}}} \quad (18)$$

$$\eta_{Comp_{PAR}} = -0.0102 R_{P,PAR}^2 + 0.0571 R_{P,PAR} + 0.5987 \quad (19)$$

Additionally, in the BFP-MSC, one more compressor consumes power (Eqn. (20,21)) in mechanical subcooling cycle.

$$\dot{W}_{Comp_{R290}} = \frac{\dot{m}_{18} * (h_{19,s} - h_{18})}{\eta_{Comp_{R290}}} \quad (20)$$

$$\eta_{Comp_{R290}} = -0.0866 R_{P,R290}^2 + 0.4521 R_{P,R290} + 0.0854 \quad (21)$$

Finally, COP value is calculated by Eqn. (22). When there is no mechanical subcooling, $\dot{W}_{Comp_{R290}}$ diminishes.

$$COP = \frac{\dot{Q}_{MT} + \dot{Q}_{LT}}{\dot{W}_{Comp_{LS}} + \dot{W}_{Comp_{HS}} + \dot{W}_{Comp_{PAR}} + \dot{W}_{Comp_{R290}} + \dot{W}_{add}} \quad (22)$$

Bin hour indicates the time spent at an ambient temperature for the period of consideration. Since hourly temperature data are obtained from the Turkish State Meteorological Service (2021) for the selected cities in the period of 2016-2020 for 5 years, bin hour values are divided by five. An annual average of the bin-hour data set is generated for dry bulb temperatures (DBT) (Fig. 4) and wet bulb temperatures (WBT) (Fig. 5). As can be seen from Fig. 4, Erzurum is the city with the lowest DBT while Mersin and Antalya attract attention with temperatures that do not fall into negative values. Diyarbakir, which has a significant amount of time at the highest temperatures, can also have values around -10 ℃. In Istanbul and Samsun, on the other hand, it is seen that the hot and cold extreme points do not take long times in a year, but middle temperatures cover significant amount of time. In Fig. 5, it is seen that the cities with the highest WBT are the ones with high humidity such as Mersin, Antalya, İzmir, Samsun, and İstanbul. Diyarbakir, which has very high DBT bin-hour data, has much lower WBT values due to the dry air of the city. As a result of dry air, Erzurum, Ankara, and Konya also spend longer times in lower WBT than other cities.

According to the bin-hour data, the amount of the time spent at the cities in four operating zones in a year are given in Fig. 6. In each city, the periods spent in subcritical regions are longer at WBT than DBT. Transcritical operating time according to WBT is only 0.16% in Antalya and 0.02% in Mersin. However, in other cities, WBT are lower than 28 ℃ which is the first operating point for Transcritical zone.

Environmental Analysis Model

Countries have targets to reduce CO_2 equivalent emissions due to international regulations (Goetzler et al., 2014). The emission values of the systems discussed in this paper should also be calculated to provide an overview to overcome the responsibilities of regulations, which Türkiye is also under obligation (Republic of Türkiye Ministry of Environment Urbanization and Climate Change, 2022).

Refrigeration systems contribute to these emissions directly due to leaks in the installation and indirectly through electricity consumption. The direct contribution depends on the total amount of refrigerant (M_{charge}), the recycling factor (α), the leaks ($M_{leakage}$), and the global warming potential (GWP) of the fluid. Indirect contribution is calculated by annual energy consumption (AEC), regional electricity conversion factor (RC) and total operation time (n). The values used in Eqn. (23,24) are given in Table 3.

$$\text{Direct Contribution} = \left(M_{leakage} n + M_{charge}(1-\alpha)\right) GWP \quad (23)$$

$$\text{Indirect contribution} = RC * AEC * n \quad (24)$$

Table 3. Parameter values in environmental analysis (Cui et al., 2020).

Parameter	Value
M_{charge} R290 (kg/kW)	2
M_{charge} CO_2 (kg/kW)	LT:3; MT:3
α	0.95
RC (kg CO_2/kWh)	0.997
GWP CO_2	1
GWP R290	3

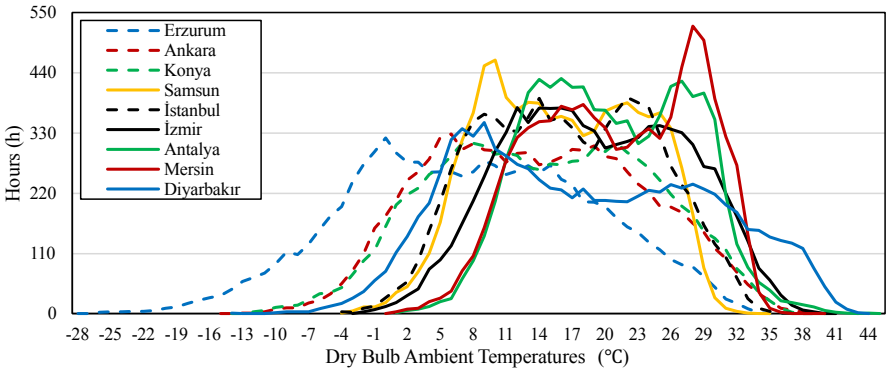

Fig. 4. Annual average DBT bin-hour values of the 9 selected cities.

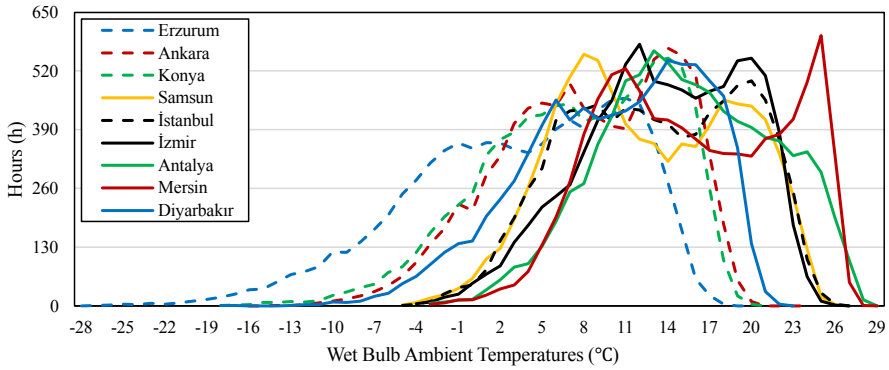

Fig. 5. Annual average WBT bin-hour values of the 9 selected cities.

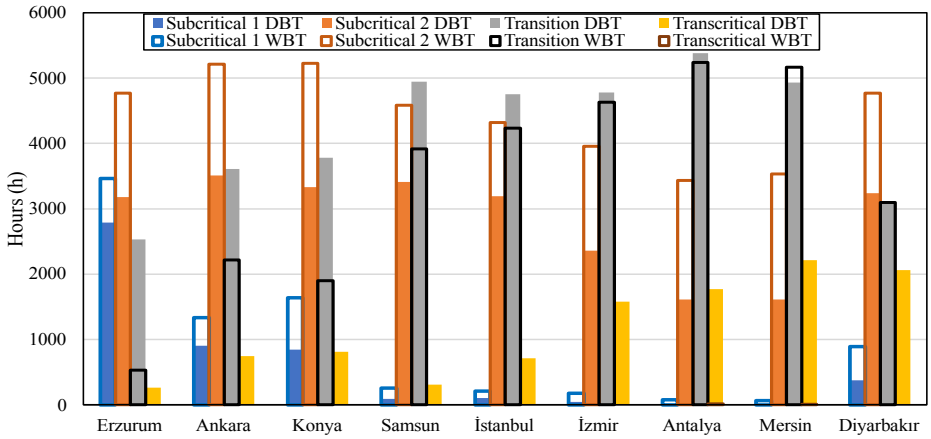

Fig. 6. Periods spent at operating zones in a year by each city.

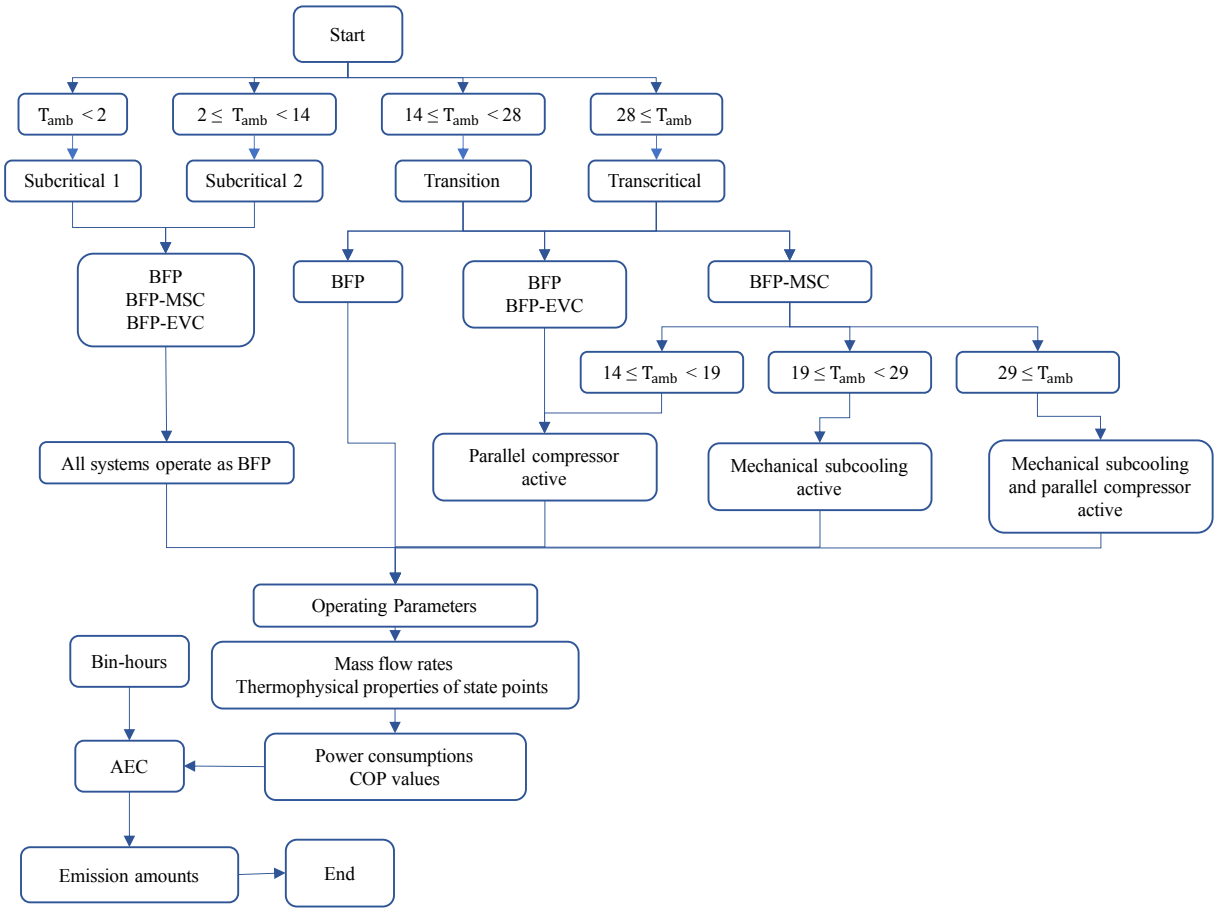

Fig. 7. Flow chart of analysis steps.

The flow chart of analyses is given in Fig. 7. Ambient temperatures at the flow chart should be considered as WBT for the BFP-EVC and DBT for others.

RESULTS AND DISCUSSION

The energy and emission analysis results of the systems whose analysis steps and assumptions are defined before are given in this section. The COP and power consumption values of the systems in question are compared and the city-oriented energy consumption values on an annual basis are presented.

Model Validation

The COP values obtained by the Engineering Equation Solver (EES) for the BFP (main system in the present study) were compared with the COP values extracted from the study of Cui et al. (2020) for the same system. Validation model was categorized into four distinct operating zones (the transcritical zone, transition zone, and two subcritical zones). Gas cooler/condenser outlet temperature and pressure values were determined according to the descriptions given in the reference paper (Cui et al., 2020).

In this validation model, the low-temperature (LT) load remained constant at 40 kW, while the medium-temperature (MT) load varies with ambient temperature. At 10°C, the MT load is 100 kW, and it linearly increases to 130 kW as the ambient temperature rises to 20°C. Beyond that, when the ambient temperature reaches 40°C, the MT load reaches its peak at 250 kW. Furthermore, LT evaporator temperature of -27°C and MT evaporator temperature of -7°C were kept fixed throughout validation. The activation of the parallel compressor occurred at 15°C ambient temperature which is a crucial parameter in the system's operation. Additionally, intermediate pressure of 3500 kPa, heat exchanger effectiveness of 0.65, and evaporator outlet quality of 0.95 were applied in validation analysis due to the assumptions of the reference paper. In this paper, the same three parameters were employed as those utilized in the reference paper chosen for validation. The average difference in COP values between the present study and the reference study was determined to be 2.33%.

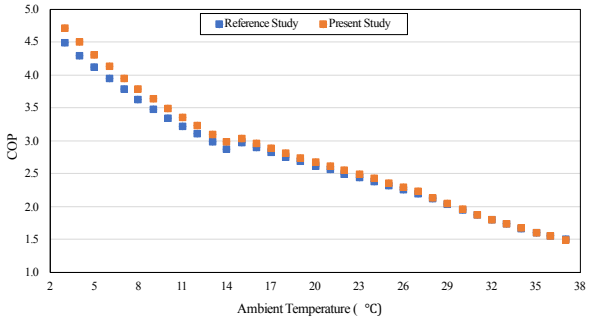

Fig. 8. COP comparison between the EES model and the study of Cui et al.(2020).

Energy Analysis Results

It has been mentioned in Energy Analysis Model section that there is an optimum gas cooler pressure value that maximizes the COP value above the critical point for CO_2 refrigeration cycles. The change of gas cooler pressure and COP value for different ambient temperatures of CO_2 booster refrigeration cycles is demonstrated in Fig. 9. A peak point on lines where COP is maximum for a specific gas cooler pressure demonstrates the optimum gas cooler pressure fact. In this study, all gas cooler pressures were optimized for each ambient temperature considered.

Within the scope of this study, there were no WBT values over 29°C available for selected Turkish cities. So, only BFP and BFP-MSC systems' COP values with respect to gas cooler pressure is presented in Fig. 9.

Fig. 10 provides valuable insights into the optimum gas cooler pressure values concerning ambient temperatures. One noteworthy observation from the data is that the optimum gas cooler pressures for the BFP consistently exceed those of the BFP-MSC across all ambient temperature conditions. It's important to note that higher gas cooler pressures can lead to increased energy consumption on compressors. This demonstrates that the utilization of mechanical subcooling enhances the performance of the BFP system. According to the meteorological data, the BFP-EVC system operates transcritical only at temperatures of 28 and 29 °C. Consequently, the optimum gas cooler pressure for this specific operating range is not shown in Fig. 10.

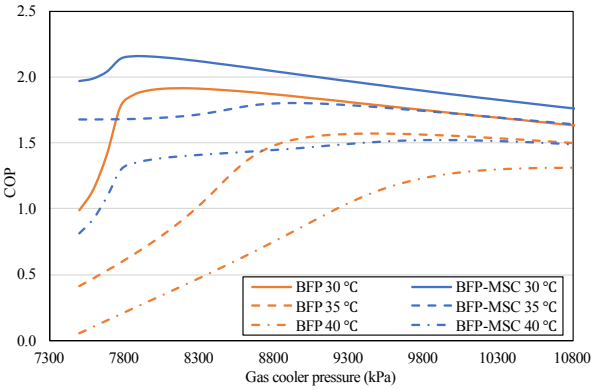

Fig. 9. Variation of COP of CO_2 booster refrigeration systems according to gas cooler pressure at different ambient temperatures.

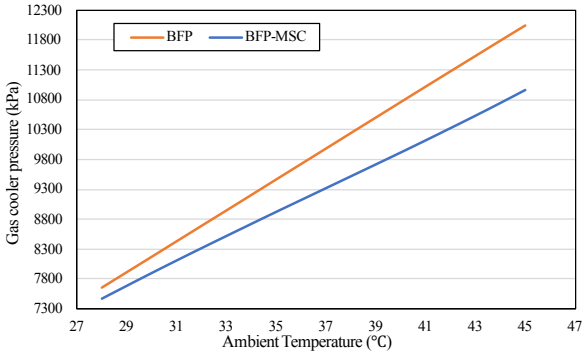

Fig. 10. Optimum gas cooler pressures with respect to ambient temperature.

Fig. 11 provides a representation of the distinct sections observed in mass flow rates, and these variations can be attributed to mechanical subcooling and the operation of parallel compressors, as indicated in Table 2. Once the parallel compressor comes into action, the HS compressor's mass flow rate is decreased to a specific value and stays constant. This reduces the work done by the HS compressor, thereby reducing total energy consumption. It becomes evident that any increase in energy consumption is primarily attributed to the influence and operation of the parallel compressor in the BFP at ambient temperatures over 14 °C. This situation is also the same for the BFP-EVC for wet bulb temperatures over 14 °C. Since the BFP and the BFP-EVC have equal mass flow rates with respect to ambient temperatures, the BFP-EVC's values were not displayed in Fig. 11 to simplify the plot. However, the ambient temperatures become wet bulb temperatures when the BFP-EVC is the system under consideration. Additionally, the mass flow rates of the LS compressor were not shown on Fig. 11 because they were constant at 0.1295 kg/s for each system under all ambient conditions.

Mass flow rates of parallel compressors are equal for BFP and BFP-MSC at 14 °C - 19 °C ambient temperature range. Above 19 °C, parallel compressor of BFP-MSC is turned off until 29 °C due to the operation of mechanical subcooling. Over 29 °C ambient temperatures, mass flow rates of parallel compressors increase with respect to ambient temperature. Additionally, BFP-MSC's parallel compressor mass flow rate is lower than BFP's parallel compressor at all ambient temperatures above 29 °C. The reason of it is the mechanical subcooling which reduces the quality of the refrigerant separated at LVS. Moreover, HS compressor's mass flow rate of BFP and BFP-MSC are equal except 19 °C - 29 °C ambient temperature range. In this temperature period, BFP-MSC system's parallel compressor is deactivated as it was previously mentioned. As a result, all the refrigerant is compressed at HS compressor at that period in BFP-MSC.

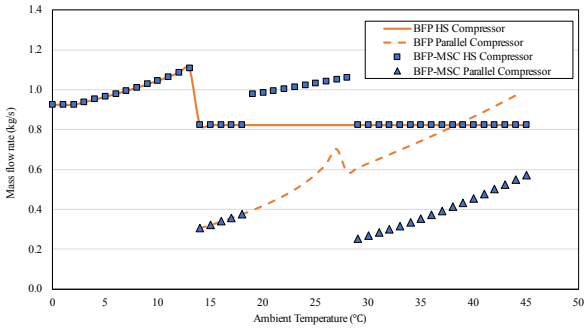

Fig. 11. Mass flow rates of HS Compressor and Parallel Compressor with respect to ambient temperature.

The variation of COP and power consumption according to the ambient temperatures for each cycle is given in Fig. 12. The performance of refrigeration systems is influenced by ambient temperature conditions. Research has consistently shown that the highest COP values are attained when the ambient temperature is at its lowest. In fact, under such conditions, the COP can reach

approximately 5. This emphasizes the efficiency of these systems when operating in colder climates. Conversely, as the ambient temperature rises, COP values exhibit a significant decline. At approximately 45 ℃ ambient temperature, the COP drops to around 1. These results align with the expected trends observed in the existing literature (Mitsopoulos et al., 2019). This inverse relationship between COP and ambient temperature highlights the critical importance of considering environmental factors in the design and operation of refrigeration systems, as well as the challenges of maintaining efficiency in warmer climates.

Since the parallel compressor is first activated at the ambient temperature of 14 °C, the COP of all systems are same below 14 ℃. The COP value of the CO_2 booster refrigeration system with flooded evaporators and parallel compressor (BFP) are up to 14.29% lower than the BFP with mechanical subcooling (BFP-MSC) at temperatures above 19 °C. When examining the COP and power consumption values of the BFP with evaporative cooling (BFP-EVC) in Fig. 12, it should be noted that the temperature values for this system are the wet bulb temperatures (WBT). The highest WBT value is 29 ℃ for investigated cities according to the meteorological data.

According to the annual energy consumption (AEC) results shown in Fig. 13, the BFP-EVC has the lowest values in each city. It has energy savings over the BFP-MSC between 8.02%-20.89%, over the BFP between 10.81%-25.47% annually. Although energy savings are achieved with the BFP-MSC compared to the BFP, this gain remained between 1.78% and 5.79%. The higher energy savings occur for the BFP-EVC because it does not operate in the transcritical region (Fig. 6). The warm cities behave like a colder city due to evaporative cooling meanwhile further savings has emerged in cities with already lower dry bulb temperatures (DBT).

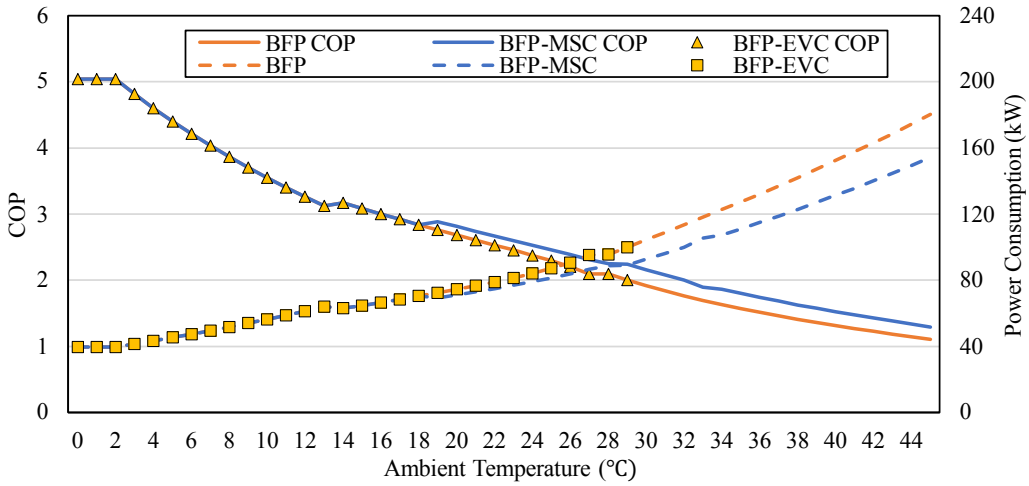

Fig. 12. COP and power consumption values with respect to ambient temperatures for systems included in this study.

When comparing results by cities, each system has the highest AEC in Mersin. Antalya, which has a similar climate to Mersin, has the second most AEC for all systems, while İzmir comes third after them. In İstanbul, Türkiye's most populated city, AEC values are 610.86 MWh for the BFP, 589.04 MWh for the BFP-MSC, and 541.01 MWh for the BFP-EVC. The lowest AEC is calculated in Erzurum.

Although the BFP-EVC is the system that consumes the least annual energy among all systems, the saving rate it provides compared to other systems differs a lot according to the cities. As seen in Fig. 14, the highest rate of savings is achieved in Diyarbakır with 25.47% and 20.89% according to the BFP and the BFP-MSC, respectively. Diyarbakır has high AEC values in systems without evaporative cooling with its high DBT. However, the humidity of this city is also low (Turkish State Meteorological Service, 2022). In this way, Diyarbakir stands out as a place where the difference between DBT and WBT is higher compared to other cities. This leads Diyarbakır to have 35.84-65.46 MWh more AEC than Samsun and İstanbul for the systems operating at DBT but 38.83-46.65 MWh lower AEC for the BFP-EVC with WBT. These results mirror those found in a study conducted in India (Lata and Gupta, 2020). The advantages of evaporative cooling are less pronounced in highly humid cities, with Ahmedabad showing a greater energy reduction compared to Chennai when employing evaporative cooling (Lata and Gupta, 2020).

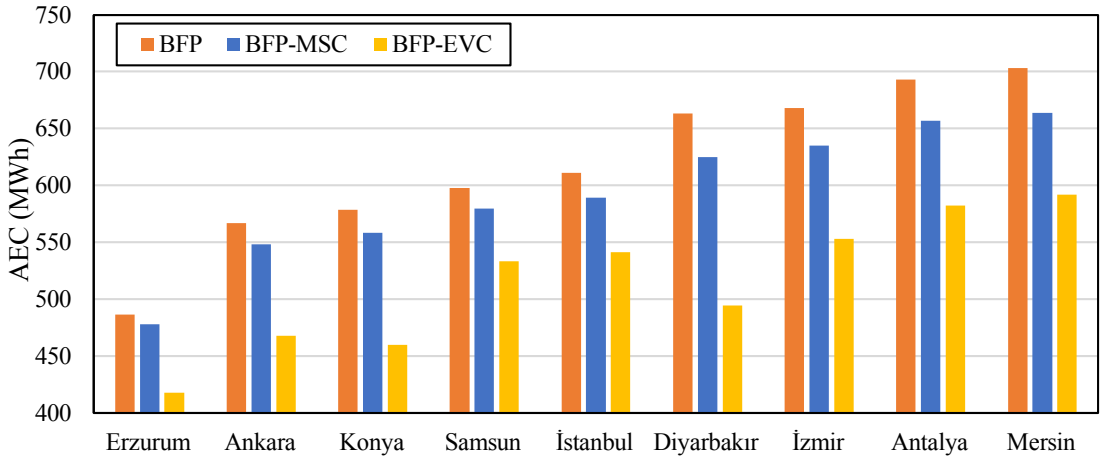

Fig. 13. AEC amounts of refrigeration systems examined according to cities

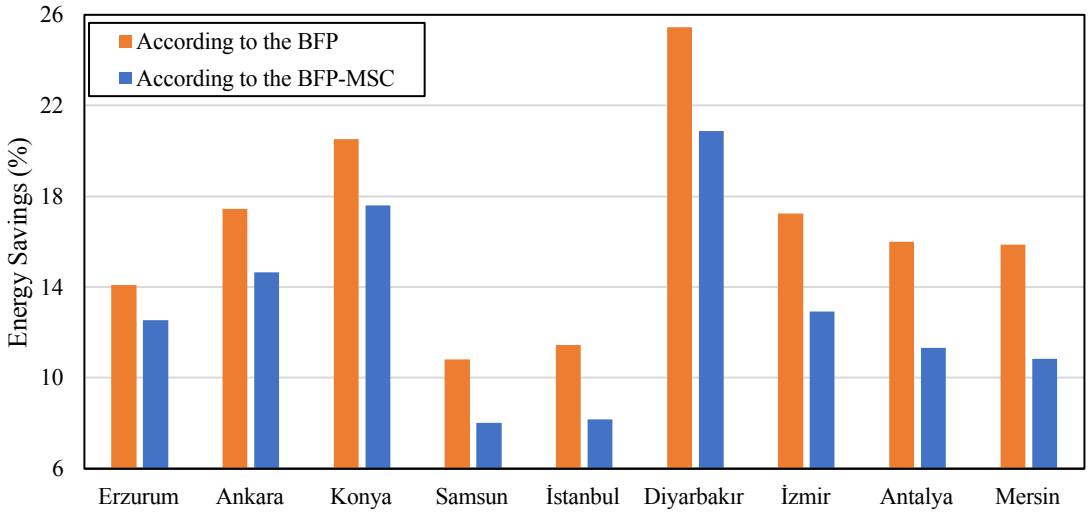

Fig. 14. Energy savings of the BFP-EVC over other systems in this study.

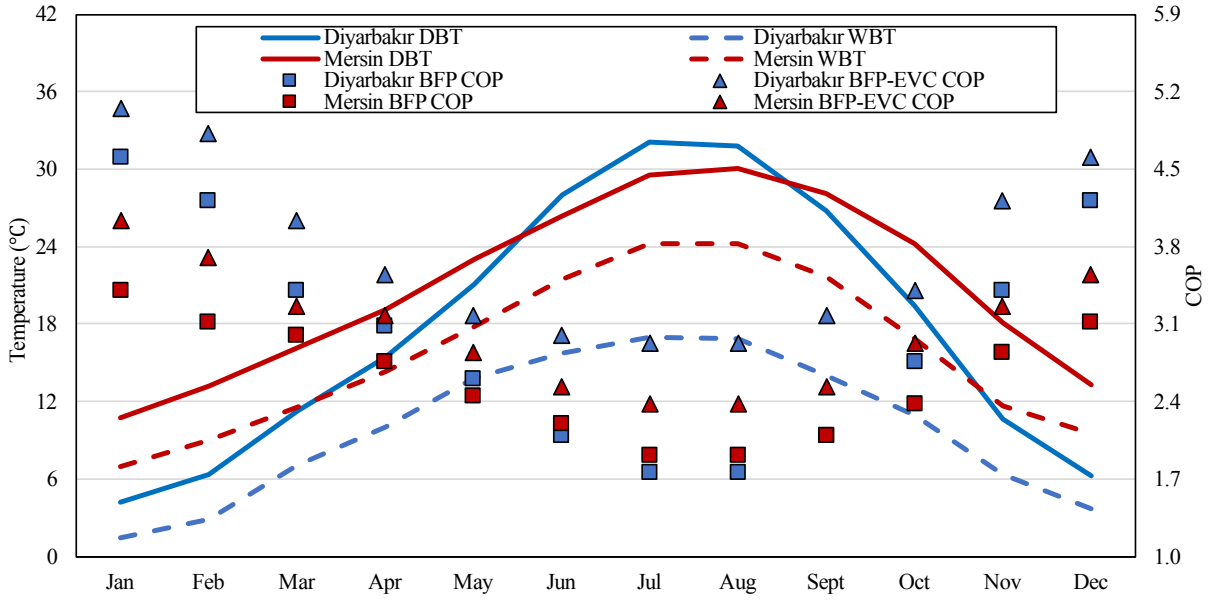

Fig. 15. Monthly average DBT, WBT, and COP values for Diyarbakır and Mersin.

Diyarbakır also has higher saving ratio with evaporative cooling in comparison to the Mediterranean cities Mersin, Antalya, and İzmir which have more humid air than Diyarbakır's. In Fig. 15, Mersin and Diyarbakır's monthly average temperature and COP values are exhibited. While Mersin's difference between DBT and WBT is similar throughout a year, this gap in Diyarbakır is increasing dramatically in summer. COP values for Diyarbakır's WBT are always higher than Mersin's. On the contrary, COP values for DBT are lower in Diyarbakır in June, July, and August.

Similarly, between Konya and Samsun, there is the AEC difference of 19.07 MWh for the BFP and 21.49 MWh for the BFP-MSC. However, the AEC difference for the BFP-EVC system is 73.21 MWh. This is because Samsun, located on the Black Sea coast, is a more humid city compared to Konya (Turkish State Meteorological Service, 2022) The difference between these two cities is also seen in Fig. 16 showing the annual duration of the COP values. Although it is clear in Fig. 16 that the WBT provides higher COP values for the BFP-EVC than other systems, it seems to have a similar time distribution pattern to the systems analyzed for DBT in Samsun. In Konya, it is seen in Fig. 16, the BFP-EVC not only has higher COP values compared to the other two systems, but also spends much more time at these COP values. A vertical line in both graphs occur since the COP value reaches its maximum and remains constant below 2°C. Konya's total bin-hour of maximum COP is also higher than Samsun's.

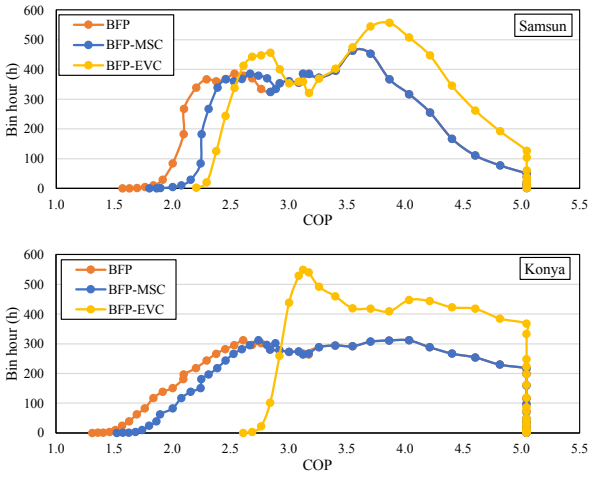

Fig. 16. Bin-hour for COP values for Samsun and Konya.

Emission Analysis Results

Total equivalent CO_2 emission values of the investigated refrigeration systems are given in Fig. 17 for each city for 5 years due to the emission reduction targets of Türkiye between 2024 and 2029 (Republic of Türkiye Ministry of Environment Urbanization and Climate Change, 2022). According to the analysis results, the BFP-EVC has fewer emissions than the BFP between 322.13 tons and 842.05 tons for 5 years of operation time.

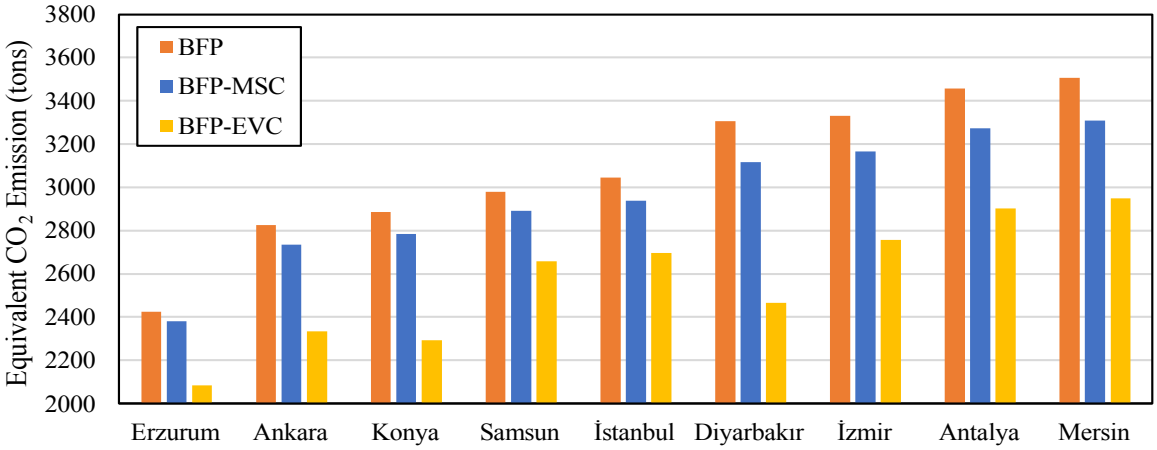

Fig. 17. CO_2 emission amounts of each refrigeration system by the city for 5 years.

CO_2 is used in all systems but only R290 is used in the mechanical subcooling cycle. Both these fluids have low global warming potential (GWP) values (Table 3). For this reason, the direct contribution of all refrigeration systems included in this study to the emission have a low share in the total (0.024%-0.033%).

As a result, the amount of emissions obtained is directly proportional to the annual energy consumptions (Fig. 13). So, the BFP-EVC's emission reduction ratios in comparison to the BFP are higher in low humidity cities as expected. These findings closely resemble those from a study conducted in China. In that study, cities with lower energy consumption also exhibited lower total equivalent CO_2 emissions, reinforcing the relationship between energy efficiency and emissions reduction (Cui et al., 2020).

CONCLUSION

Energetic and environmental analyses of the CO_2 booster refrigeration cycle with the flooded evaporators and parallel compressor (BFP), the CO_2 booster refrigeration system with the flooded evaporators, parallel compressor and mechanical subcooling (BFP-MSC) and the CO_2 booster refrigeration system with the flooded evaporators, parallel compressor and evaporative cooling

(BFP-EVC) were performed for nine cities in Türkiye for the first time in literature.

According to the results, these conclusions can be made:

- The primary factor contributing to energy savings is the reduction in mass flow rate achieved through the implementation of mechanical subcooling and a parallel compressor.
- COP of the CO_2 booster refrigeration systems increases at low ambient temperatures.
- COP of the BFP-MSC is up to 16.67% higher than the BFP for the same dry bulb temperatures.
- Annual energy consumption (AEC) of the BFP-EVC is the lowest for each city up to 25.47%.
- In comparison of AEC, the BFP-MSC and the BFP follow the BFP-EVC in each city, respectively.
- Evaporative cooling provides less energy saving ratio in cities with higher humidity.
- CO_2 emission amounts are directly proportional to the AEC due to the low GWP of CO_2 and R290.
- The highest AEC is obtained in Mersin and the lowest in Erzurum for all systems.
- According to the analysis results, it is recommended for all the cities to use the BFP-EVC.

REFERENCES

Amaris, C., Tsamos, K. M., and Tassou, S. A., 2019, Analysis of an R744 typical booster configuration, an R744 parallel-compressor booster configuration and an R717/R744 cascade refrigeration system for retail food applications. Part 1: Thermodynamic analysis. *Energy Procedia,* 161, 259–267. https://doi.org/10.1016/j.egypro.2019.02.090

Atmaca, A. U., Erek, A., Ekren, O., and Çoban, M. T., 2018, Thermodynamic Performance of the Transcritical Refrigeration Cycle with Ejector Expansion for R744, R170, and R41. *J. of Thermal Science and Technology,* 38, 111–127.

Bayrakçı, H. C., Özgür, A. E., and Alan, A., 2014, Çift Kademeli Transkritik R744 Soğutma Sistemlerinde Genleşme Türbini Kullanımının Termodinamik Analizi. *J. of Thermal Science and Technology,* 34, 91–97.

Caliskan, O., and Ersoy, H. K., 2022, Energy analysis and performance comparison of transcritical CO2 supermarket refrigeration cycles. The Journal of *Supercritical Fluids,* 189, 105698. https://doi.org/10.1016/j.supflu.2022.105698

Chesi, A., Esposito, F., Ferrara, G., and Ferrari, L., 2014, Experimental analysis of R744 parallel compression cycle. *Applied Energy,* 135, 274–285. https://doi.org/10.1016/j.apenergy.2014.08.087

Cui, Q., Gao, E., Zhang, Z., and Zhang, X., 2020, Preliminary study on the feasibility assessment of CO2 booster refrigeration systems for supermarket application in China: An energetic, economic, and environmental analysis. *Energy Conversion and Management*, 225. https://doi.org/10.1016/j.enconman.2020.113422

Dai, B., Cao, Y., Liu, S., Ji, Y., Sun, Z., Xu, T., Zhang, P., and Nian, V., 2022, Annual energetic evaluation of multi-stage dedicated mechanical subcooling carbon dioxide supermarket refrigeration system in different climate regions of China using genetic algorithm. Journal of *Cleaner Production,* 333. https://doi.org/10.1016/j.jclepro.2021.130119

Ersoy, H. K., and Bilir, N., 2012, Performance characteristics of ejector expander transcritical CO2 refrigeration cycle. *Proceedings of the Institution of Mechanical Engineers, Part A: Journal of Power and Energy,* 226(5), 623–635. https://doi.org/10.1177/0957650912446547

European Commission, 2008, Development and demonstration of a prototype transcritical CO_2 refrigeration system Final Report.

Fricke, B., Zha, S., Sharma, V., Newel, J., and Sharma, V., 2016, Laboratory Evaluation of a Commercial CO_2 Booster Refrigeration System Laboratory Evaluation of a Commercial CO2 Booster Refrigeration System. *International Refrigeration and Air Conditioning Conference. Paper 1691.* http://docs.lib.purdue.edu/iracc/1691

Fritschi, H., Tillenkamp, F., Löhrer, R., and Brügger, M., 2017, Efficiency increase in carbon dioxide refrigeration technology with parallel compression. International *Journal of Low-Carbon Technologies*, 12(2), 171–180. https://doi.org/10.1093/ijlct/ctw002

Ge, Y. T., Tassou, S. A., Santosa, I. D., and Tsamos, K., 2015, Design optimisation of CO2 gas cooler/condenser in a refrigeration system. *Applied Energy*, 160, 973–981. https://doi.org/10.1016/j.apenergy.2015.01.123

Goetzler, W., Sutherland, T., Rassi, M., and Burgos, J., 2014, Research and Development Roadmap for Next-Generation Low Global Warming Potential Refrigerants. www.osti.gov/home/

Gullo, P., Cortella, G., Minetto, S., and Polzot, A., 2016, Overfed evaporators and parallel compression in commercial R744 booster refrigeration systems - An assessment of energy benefits. *Refrigeration Science and Technology,* 261–268. https://doi.org/10.18462/iir.gl.2016.1039

Gullo, P., and Hafner, A., 2017, Thermodynamic performance assessment of a CO2 supermarket refrigeration system with auxiliary compression economization by using advanced exergy analysis. *International Journal of Thermodynamics*, 20(4), 220–227. https://doi.org/10.5541/ijot.325883

Gullo, P., Hafner, A., and Banasiak, K., 2018, Transcritical R744 refrigeration systems for supermarket applications: Current status and future perspectives. In

International Journal of Refrigeration, 93, 269–310. https://doi.org/10.1016/j.ijrefrig.2018.07.001

ICF Incorporated, 2020, Supermarket Emission Reduction Analysis.

Işık, M., 2022, Thermodynamic Analysis of CO2 Booster Refrigeration Systems of Supermarket Applications for Türkiye [MSc Thesis]. Konya Technical University Graduate Education Institute.

Işık, M. and Bilir Sağ, N., 2023, Energetic, economic, and environmental analysis of CO2 booster refrigeration systems of supermarket application for Türkiye. *Sadhana*, 48, 275, https://doi.org/10.1007/s12046-023-02337-3

Karampour, M., and Sawalha, S., 2018, State-of-the-art integrated CO2 refrigeration system for supermarkets: A comparative analysis. *International Journal of Refrigeration*, 86, 239–257. https://doi.org/10.1016/j.ijrefrig.2017.11.006

Kauf, F., 1999, Determination of the optimum high pressure for transcritical CO2-refrigeration cycles. *International Journal of Thermal Sciences*, 38, 325–330.

Lata, M., and Gupta, D. K., 2020, Performance evaluation and comparative analysis of trans-critical CO2 booster refrigeration systems with modified evaporative cooled gas cooler for supermarket application in Indian context. *International Journal of Refrigeration*, 120, 248–259. https://doi.org/10.1016/j.ijrefrig.2020.08.004

Lata, M., Purohit, N., and Gupta, D. K., 2021, Techno-economic assessment of trans-critical CO2 booster system with modified evaporative cooling for supermarket application in Indian context. *Environmental Progress and Sustainable Energy*, 40(2). https://doi.org/10.1002/ep.13551

Liao, S. M., Zhao, T. S., and Jakobsen, A., 2000, A correlation of optimal heat rejection pressures in transcritical carbon dioxide cycles. *Applied Thermal Engineering*. www.elsevier.com/locate/apthermeng

Llopis, R., Cabello, R., Sánchez, D., and Torrella, E., 2015, Energy improvements of CO2 transcritical refrigeration cycles using dedicated mechanical subcooling. *International Journal of Refrigeration*, 55, 129–141. https://doi.org/10.1016/j.ijrefrig.2015.03.016

Llopis, R., Sanz-Kock, C., Cabello, R., Sánchez, D., and Torrella, E., 2015, Experimental evaluation of an internal heat exchanger in a CO2 subcritical refrigeration cycle with gas-cooler. *Applied Thermal Engineering*, 80, 31–41.https://doi.org/10.1016/j.applthermaleng.2015.01.040

Mitsopoulos, G., Syngounas, E., Tsimpoukis, D., Bellos, E., Tzivanidis, C., and Anagnostatos, S., 2019, Annual performance of a supermarket refrigeration system using different configurations with CO2 refrigerant. *Energy Conversion and Management: X*, 1. https://doi.org/10.1016/j.ecmx.2019.100006

Mylona, Z., Kolokotroni, M., Tsamos, K. M., and Tassou, S. A., 2017, Comparative analysis on the energy use and environmental impact of different refrigeration systems for frozen food supermarket application. *Energy Procedia*, 123, 121–130. https://doi.org/10.1016/j.egypro.2017.07.234

Nebot-Andrés, L., Sánchez, D., Calleja-Anta, D., Cabello, R., and Llopis, R., 2021, Experimental determination of the optimum intermediate and gas-cooler pressures of a commercial transcritical CO2 refrigeration plant with parallel compression. *Applied Thermal Engineering*, 189. https://doi.org/10.1016/j.applthermaleng.2021.116671

Özgür, A. E., Bayrakçı, H. C., and Akdağ, A. E., 2009, Kritik Nokta Üstü Çevrimli CO2 Soğutma Sistemlerinde Optimum Gaz Soğutucu Basıncı: Yeni Bir Korelasyon The Optimum Gas Cooler Pressure for Transcritical CO2 Refrigeration Cycle: a New Correlation. *J. of Thermal Science and Technology*, 29, 23–28.

Purohit, N., Gupta, D. K., and Dasgupta, M. S., 2017, Energetic and economic analysis of trans-critical CO2 booster system for refrigeration in warm climatic condition. *International Journal of Refrigeration,* 80, 182–196. https://doi.org/10.1016/j.ijrefrig.2017.04.023

Republic of Türkiye Ministry of Environment Urbanization and Climate Change, 2022, Montreal Protocol. https://iklim.csb.gov.tr/montreal-protokolu-i-4364

Sacasas, D., Vega, J., and Cuevas, C., 2022, An annual energetic evaluation of booster and parallel refrigeration systems with R744 in food retail supermarkets. A Chilean perspective. *International Journal of Refrigeration*, 133, 326–336. https://doi.org/10.1016/j.ijrefrig.2021.10.010

Sarkar, J., and Agrawal, N., 2010, Performance optimization of transcritical CO2 cycle with parallel compression economization. *International Journal of Thermal Sciences*, 49(5), 838–843. https://doi.org/10.1016/j.ijthermalsci.2009.12.001

Sawalha, S., 2008a, Theoretical evaluation of trans-critical CO2 systems in supermarket refrigeration. Part I: Modeling, simulation and optimization of two system solutions. *International Journal of Refrigeration*, 31(3), 516–524. https://doi.org/10.1016/j.ijrefrig.2007.05.017

Sawalha, S., 2008b, Theoretical evaluation of trans-critical CO2 systems in supermarket refrigeration. Part II: System modifications and comparisons of different solutions. *International Journal of Refrigeration*, 31(3), 525–534. https://doi.org/10.1016/j.ijrefrig.2007.05.018

Sooben, D., Purohit, N., Mohee, R., Meunier, F., and Dasgupta, M. S., 2019, R744 refrigeration as an alternative for the supermarket sector in small tropical island developing states: The case of Mauritius. *International Journal of Refrigeration*, 103, 264–273. https://doi.org/10.1016/j.ijrefrig.2019.03.034

Sun, Z., Li, J., Liang, Y., Sun, H., Liu, S., Yang, L., Wang, C., and Dai, B., 2020, Performance assessment of CO2 supermarket refrigeration system in different climate zones of China. *Energy Conversion and Management*, 208. https://doi.org/10.1016/j.enconman.2020.112572

Tsamos, K. M., Ge, Y. T., Santosa, Id., Tassou, S. A., Bianchi, G., and Mylona, Z., 2017, Energy analysis of alternative CO2 refrigeration system configurations for retail food applications in moderate and warm climates. *Energy Conversion and Management*, 150, 822–829. https://doi.org/10.1016/j.enconman.2017.03.020

Turkish State Meteorological Service, 2021, Meteorological Data.

Turkish State Meteorological Service, 2022, Climate Assessment of 2021. https://www.mgm.gov.tr